Current Opinion in Colloid & Interface Science 18 (2013) 432–439

Contents lists available at ScienceDirect

Current Opinion in Colloid & Interface Science

journal homepage: www.elsevier.com/locate/cocis

# Physics of interactions at biological and biomaterial interfaces ☆

Motomu Tanaka *

*Physical Chemistry of Biosystems, Institute of Physical Chemistry, University of Heidelberg, D69120 Heidelberg, Germany*
*Institute for Integrated Cell-Material Science (iCeMS), Kyoto University, 606-8501 Kyoto, Japan*

ARTICLE INFO

*Article history:*
Received 28 May 2013
Received in revised form 1 July 2013
Accepted 2 July 2013
Available online 10 July 2013

*Keywords:*
Supported membrane
Grazing incidence
X-ray fluorescence
Offspecular scattering
Cell adhesion
Cell migration

ABSTRACT

Soft interlayers based on membranes and biopolymers define the spatial boundaries between different phases in biological systems. Physical interactions of soft matter under biologically relevant conditions (in aqueous media containing various ions) are governed by complex interplays of generic and specific interfacial interactions, which are clearly different from those acting at the interface between hard matter. This review aims at providing a comprehensive overview on: (a) models of cell–cell and cell–tissue interfaces with aid of defined building blocks, (b) new X-ray and neutron scattering techniques to probe fine structures, electrostatics, and mechanics of soft interfaces, and (c) control of dynamic cell morphology and migration of cells using tailor-made, soft interfaces.



## 1. Introduction

In biological systems, boundaries between many phases are defined by "soft interlayers", such as membranes and biopolymers, which are immersed in physiological electrolytes. For example, biological membranes are vital components that define the outer boundary of living cells to the surrounding environments as well as that of cell compartments (organelles) in cytoplasmic space. Their main constituent is a bilayer lipid membrane that sustains lateral fluidity, and a variety of membrane-associated proteins facilitate communication and transport on/across the membrane. From the view point of material science, membranes serve as smart filters that confine many processes in the compartments (organelles). Here, toxic substances are kept out of the cell, while specific nutrients, wastes and metabolites can pass across the membranes to reach their destinations. On the other hand, if one sheds light on membranes from a biochemical point of view, many important biological processes are regulated at membrane surfaces, through interactions between peripheral and integral membrane proteins.

### 1.1. Importance of interfaces in biological systems

Why does nature need/use interfaces? In the 70's, Hardt [1] showed a relatively simple answer to the question by extending the steady state of diffusion-limited reactions described by Smoluchowski, and represented the mean diffusion time $\tau$ for three body collision in two- and three-dimensions:

$$\langle \tau_{2D} \rangle = \frac{x^2}{2D} \ln\left(\frac{x}{r}\right) \text{ and } \langle \tau_{3D} \rangle = \frac{x^3}{3Dr}. \quad (1)$$

$D$ is the diffusion coefficient, $r$ the radius of diffusing particles, and $x$ the separation distance between two particles. The dependence of mean diffusion time on the particle radius $r$ is $\langle \tau_{2D} \rangle \propto -\ln(r)$ for two-dimensional systems, while $\langle \tau_{3D} \rangle \propto r^{-1}$ in three-dimensional systems. A clear difference in the dependence of $\tau$ on $r$ indicates the energetic and thus economic reasons why many biochemical reactions are confined in 2D membranes.

### 1.2. Free energy minimization by soft interfaces

As a general starting point, let us consider interactions between two biological interfaces (e.g. two neighboring cell membranes) as those between two planes that keep a finite separation distance via a thin spacer. When a separation distance is large, the interlayer retains its intrinsic bulk properties. Here, a change in the interlayer thickness at a constant phase volume does not cost any energy penalty, as all individual interfaces follow the classical Gibbs capillary theory. In contrast, any change in the interlayer thickness costs energy if the long-range force fields overlap within interlayers.

In order to analytically describe the thermodynamics of thin liquid films, Derjaguin introduced a simple measure, called disjoining pressure [2]. Disjoining pressure $\Pi$ is defined as the excess of the external pressure that must be applied to the fluid interlayer between the plates



* Physical Chemistry of Biosystems, Institute of Physical Chemistry, University of Heidelberg, D69120 Heidelberg, Germany. Tel.: +49 6221544916.
*E-mail address:* tanaka@uni-heidelberg.de.

1359-0294/$ – see front matter © 2013 The Author. Published by Elsevier Ltd. All rights reserved.
http://dx.doi.org/10.1016/j.cocis.2013.07.002

in order to keep a finite distance. Practically, $\Pi$ is nothing but the sum of the all individual forces acting per unit area, which can experimentally be determined by measuring the external pressures to keep the separation distance constant. The disjoining pressure can be defined in terms of the lateral density of Gibbs free energy at constant temperature $T$: $\Pi(d) = -(\partial G/\partial d)_T$, where $d$ is the interlayer thickness (Fig. 1).

In order to keep a finite separation distance $d$ between two planes, the free energy minimization coincides with the condition of $\Pi = 0$. When the interaction is weak, the interfacial interaction potential $V(d)$ can be approximated by a harmonic potential according to the inverse work functional theory as the probability function of the spacing distance follows the Boltzmann distribution: $V(d) \propto -kT \ln P(d)$.

On the other hand, the continuous thinning of the interlayer results in collapse/dewetting of the interlayer. Typical examples in material science are the rupturing of polymer and surfactant films [3,4].

## 2. Model cell membranes on soft surfaces: "polymer-supported membranes"

As experimental models of cell surfaces, phospholipid bilayers deposited onto planar solid substrates (so-called "solid-supported membranes") have commonly been used for almost 30 years [5••,6••,7]. Supported membranes retain both the lateral fluidity and excellent mechanical stability. They do not only enable one to probe the structural and dynamic properties of membranes with various surface-sensitive techniques, but also allow for in vitro modeling of cell–cell recognition. Solid-supported membranes have the drawback of being confined in the close proximity of solid substrates. Here, the separation via a very thin water reservoir (thickness: 5–20 Å) is not sufficient to prevent large transmembrane proteins from coming into direct contact with the bare substrate.

This problem can be avoided by separating membranes and solid substrates using soft interlayers based on hydrated polymers [8••,9]. In nature, interactions between cells and tissues are mediated by complex interplays of short-range and long-range forces across hydrated layers of carbohydrate-based biopolymers, such as extracellular matrix and cell surface glycocalyx. They keep a finite distance (typically in the range of 10–100 nm) between neighboring cells to avoid direct, non-specific cell–cell contacts as well as to create hydrodynamic pathways for solute transport.

### 2.1. Roles of soft interfaces (1): wetting, lateral fluidity

The deposition of a lipid bilayer onto a hydrated polymer support can energetically be favored only if the presence of a membrane results in the gain of Gibbs free energy of the whole system. For example, the stability of a liquid film on a surface can be characterized by a spreading coefficient $S$ within the basic framework of wetting physics: [10] $S = \gamma_{SV} - (\gamma_{SL} + \gamma_{LV})$. Here, $\gamma_{SV}$ is the free energy of the solid/vapor interface, $\gamma_{SL}$ at solid/liquid interface, and $\gamma_{LV}$ liquid/vapor interface. Compared to solid-supported membranes, the presence of polymer supports assists the self-healing of local defects in the membrane to cover macroscopically large substrates (~cm$^2$) [11].

Within the framework of Saffman and Delbrück's approach [12••], the translational diffusion coefficient of a cylindrical particle (radius $R_p$) immersed in a quasi-2D continuum is written as:

$$D \sim \frac{k_B T}{4\pi\eta_m h} \ln\left(\frac{\eta_m h}{\eta_w R_p} - \gamma\right). \tag{2}$$

$\eta_w$ and $\eta_m$ are the viscosities of medium (water) and membrane given in [Pa s], $h$ the thickness of membrane and hence the height of a particle, and $\gamma$ Euler's constant $\gamma = 0.5772$. Such a logarithmic law suggests a relatively little dependence of $D$ on the particle radius $R_p$, which agrees well with experimental findings [13].

To model the lateral diffusion lipids and proteins in contact with viscous, asymmetric environments (e.g. glycocalyx and cytoskeleton), it is necessary to consider asymmetric boundary conditions (Fig. 2). Evans and Sackmann [14] expressed the diffusion coefficient $D$ as a function of the dimensionless particle radius of diffusing particle $\varepsilon$:

$$D = \frac{kT}{4\pi\eta_m h}\left(\frac{1}{4}\varepsilon^2 + \frac{\varepsilon K_1(\varepsilon)}{K_0(\varepsilon)}\right)^{-1}. \tag{3}$$

$K_0$ and $K_1$ are modified zero and first order Bessel functions of the second kind. In contrast to the description in Eq. (2), the diffusion constant is much more strongly dependent on the particle size. It should be noted that $\varepsilon$ can analytically be obtained from the dimensionless particle mobility $m = 4\pi\eta_m D/k_B T$, which can be determined from the diffusion coefficient $D$. The frictional coefficient $b_s$ can be given by the membrane viscosity $\eta_m$, membrane thickness $h$, and the ratio between $\varepsilon$ and the radius of transmembrane domain $R_p$: $b_s = \eta_m h(\varepsilon/R_p)^2$. Namely, once $R_p$ is known, one can determine the significance of frictional stress exerted on proteins. This enables one to nail down how the thickness and density of polymer interlayers influence the friction exerted on transmembrane receptor proteins in a quantitative manner [15•].

### 2.2. Roles of soft interfaces (2): modulation of interfacial forces

If one takes lipids and polymers that carry no net charges (e.g. zwitter-ionic lipids and neutral polymer chains, Fig. 3a), one can identify the three major long-range forces (pressures) that dominate

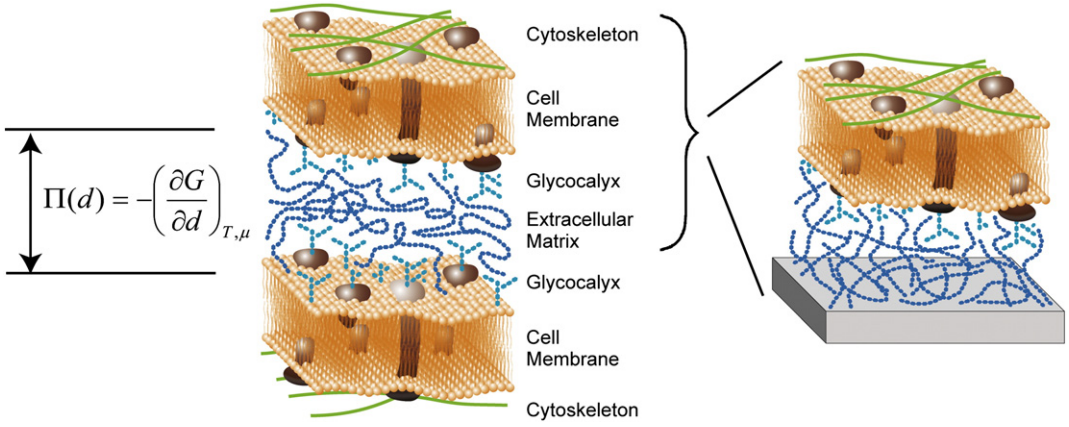


**Fig. 1.** Models of cell–extracellular matrix contacts by the deposition of a two-dimensional cell membrane on a polymer support (polymer-supported membrane). The net force acting per unit area (disjoining pressure) coincides with the excess pressure to maintain the finite distance between two planes.

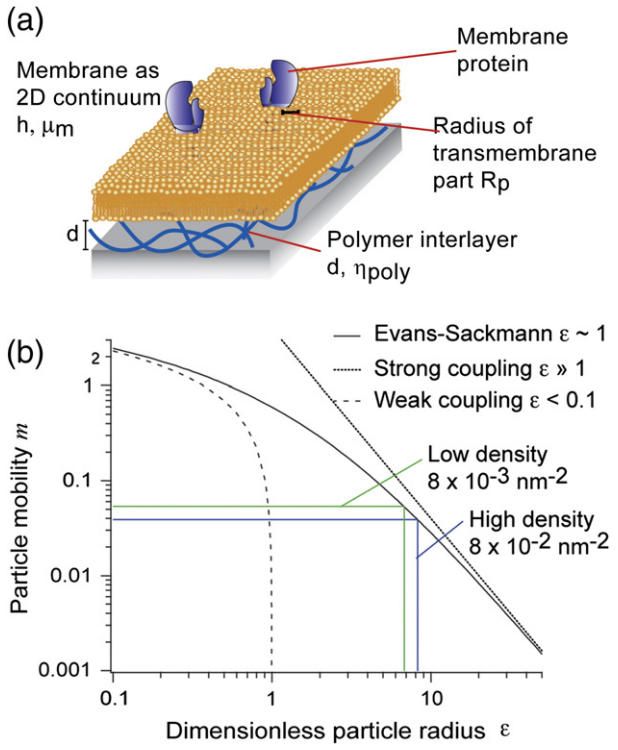


**Fig. 2.** (a) Lateral diffusion of membrane proteins in a supported membrane. The frictional coupling between a cylindrical particle and the substrate is modulated by the presence of a soft interlayer. (b) Particle mobility plotted as a function of dimensionless particle radius within the frameworks of (i) the Saffman–Delbrück's continuum model ($\varepsilon < 0.1$), (ii) the strongly coupled model ($\varepsilon > 0.1$), and (iii) the modified theory derived by Evans and Sackmann. The experimental results from integrin receptors in polymer-tethered membranes at low and high tether densities can be well explained by the Evans–Sackmann model.

interfacial interactions: (a) van der Waals pressure, (b) hydration repulsion, and (c) undulation repulsion originating from the thermodynamic fluctuation of the membrane.

First, the van der Waals pressure in the presence of a polymer interlayer can be calculated on the basis of an asymmetric five layer model as a function of interlayer thickness $d$ [16]. If one takes a silicon wafer as a substrate, layer 1 and 2 are the bulk crystalline silicon and silicon dioxide (thickness $T_1$), respectively. Layer 3 consists of the polymer spacer, layer 4 is the lipid membrane with thickness $T_2$ and layer 5 is bulk water. With this model, $P_{vdW}(d)$ can be written as:

$$P_{vdW}(d) = \frac{1}{6\pi}\left(\frac{A_{234}}{d^3} - \frac{\sqrt{A_{121}A_{343}}}{(d+T_1)^3} - \frac{\sqrt{A_{545}A_{323}}}{(d+T_2)^3} - \frac{\sqrt{A_{545}A_{121}}}{(d+T_1+T_2)^3}\right). \quad (4)$$

$A_{ijk}$ stands for the Hamaker constant of medium i interacting with medium j through medium k.

The second, hydration pressure $P_{hyd}(d)$ [17••], is a consequence of the work necessary for removing water from a hydrated layer to the infinitely thick, bulk liquid phase. $P_{hyd}(d)$ exponentially decays over a distance, parameterized by a pressure constant $P_0$ and a characteristic decay constant $\lambda_H$: $P_{hyd}(d) = P_0 \exp(-d/\lambda_H)$. The values for $P_0$ and $\lambda_H$ can be obtained by measuring the equilibrium thicknesses of the polymer layer at different osmotic pressures.

The repulsive pressure originating from thermodynamic undulations [18••,19] adjacent to the wall $P_{und}(d)$ is given as a function of the bending rigidity of membrane $\kappa$:

$$P_{und}(d) = \alpha_1 \frac{(k_B T)^2}{\kappa d^3}. \quad (5)$$

As presented in Fig. 3b, the generic roles of polymer interlayers in modulating the membrane–substrate contact can be verified by comparing the calculated equilibrium distance by extrapolation of the sum of three forces to zero (blue bar) and the membrane–substrate distance experimentally determined by elliposometry and specular X-ray reflectivity (red bar) [20]. This suggests that the balance between attractive van der Waals pressure and hydration repulsion play dominant roles in stabilizing membranes at finite distances from underlying substrates.

### *2.3. Two-dimensional cell membranes: soft interface facilitates complete wetting*

Polymer supported membranes enable proteins to fully retain their mobility and native functionality. For example, when probing the interaction between polymer-supported membranes incorporating integrin receptors and giant vesicles exposing specific ligand molecules, the adhesion free energy and thus the binding energy for the interaction is comparable to the value inferred from the integrin–ligand dissociation constant. However, the orientation and the population of transmembrane proteins in native cell membranes are stringently controlled,

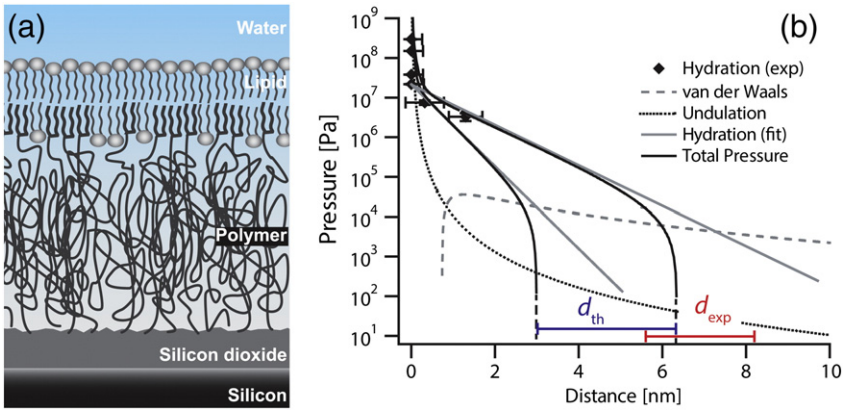


**Fig. 3.** (a) A schematic illustration of a "polymer-tethered" membrane incorporating lipids with linear polymer head groups. (b) The calculated force–distance curves of the polymer-tethered membrane: van der Waals pressure is indicated by broken gray line and thermal fluctuation by a dotted line. The hydration pressure can be obtained by fitting the experimental data. The error range is indicated by two fitting curves (solid gray lines). The sum of three forces yields disjoining pressures (black solid lines). The extrapolation to $P = 0$ predicts the equilibrium distance $d_{th}$ (blue bar), showing a reasonable agreement with the experimentally determined equilibrium membrane–substrate distance (red bar). Note that van der Waals pressure is displayed with opposite sign in the panel.

and it is difficult to incorporate complex and concentrated protein mixtures into supported membranes.

This can be overcome by spreading native cell membrane extracts onto planar substrates, which has first been demonstrated by the deposition of human erythrocyte "ghost cells" (after removal of intracellular components) on 10 nm thick, hydrated cellulose cushions [21•]. As described in the previous session, the formation of defect-free membranes that selectively expose the cytoplasmic surface can be attributed to the fine adjustment of interface tensions (wetting condition) and the balance of interfacial forces acting in the direction perpendicular to the membrane surface (Fig. 4a). By contrast, the deposition of cell membranes on positively charged polyelectrolyte films results in the pinning of membrane patches, which can be interpreted as the dewetting caused by too strong electrostatic attractions (Fig. 4b). This suggests that the use of highly charged polyelectrolytes as polymer support [22,23] is feasible for synthetic lipid membranes but not for native cell membranes. In fact, even the fabrication of cell membrane arrays is possible by introducing "wetting contrasts" either by lithographic micro-patterning of polymer supports or by "stamping" proteins on polymer supports [24].

## 3. Interfacial interactions via membrane-anchored glycans

A variety of carbohydrates are covalently anchored to the head groups of lipids (e.g. phosphatidylinosytol, ganglioside, etc.) and proteins (glycoproteins) on the outer surface of biological cells [25]. These saccharide moieties serve not only as mechanical stabilizers sustaining the structural integrity of cell membranes but also as specific ligands for various receptor proteins (e.g. lectin family) in various inter-cellular communications. In fact, after the era of genomics and proteomics, the systems and integrated strategy to understand the structure–function relationships in glycans (called "glycomics") is a newly emerging scientific field [26]. However, despite significant progresses from chemical biology and system biology approaches, physics of glycans is still poorly understood.

### 3.1. Physical roles glycans (1): structures and electrostatics

Glycans on the outer surfaces of bacteria, such as lipopolysaccharides (LPSs) of Gram-negative bacteria, protect the membrane against chemical attacks by cationic antibacterial peptides (CAPs) and antibacterial drugs. Since many in-vivo studies demonstrated that divalent cations ($Ca^{2+}$, $Mg^{2+}$) significantly increase the survival rate of bacteria [27], it is highly important to study the influence of mono- and divalent ions on the fine-structures and electrostatics of glycans.

To highlight the roles of glycans, monolayers of lipopolysaccharides from various bacteria strains at the air/water interface are a defined, biologically relevant model of bacterial outer membranes. The fine-structures of LPS monolayers perpendicular to the membrane surface can be gained either by specular X-ray reflectivity (XRR) or by grazing incidence X-ray scattering out of specular plane (GIXOS) (Fig. 5a)

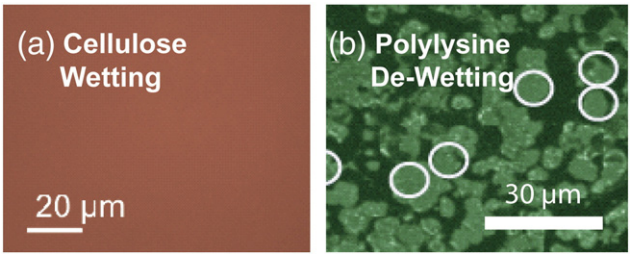


**Fig. 4.** A native supported membrane spread on a polymer support. (a) Immunofluorescence staining of a human erythrocyte membrane with the antibody to the cytoplasmic domain of Band III denotes the exposure of the "inside" to the bulk. (b) The corresponding image on a cationic polyelectrolyte (polylysine) support suggests strong attractions cause the "de-wetting" of cell membranes.

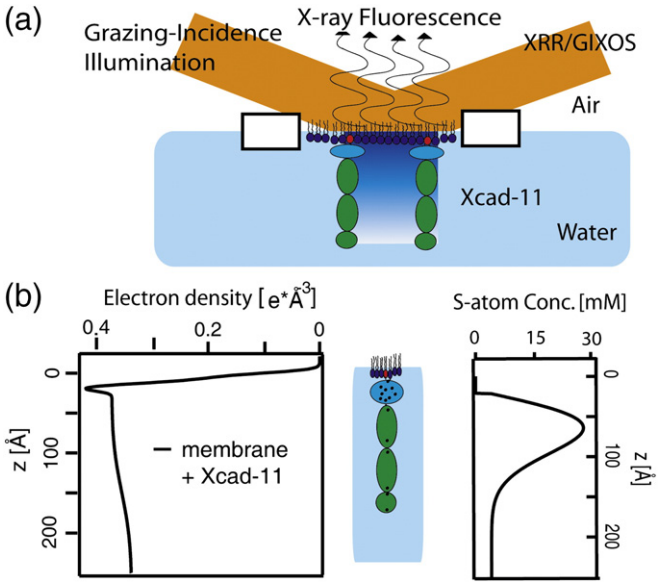


**Fig. 5.** (a) Schematic illustration of GIXF and XRR/GIXOS setup. (b) The electron density profiles reconstructed from XRR/GIXOS results, while concentration profiles from target elements (in this case, S-atom from recombinant cadherin) can be calculated from GIXF. Note that precise determination of electron density profiles from XRR/GIXOS is necessary for quantitative GIXF analysis.

[28•]. In GIXOS measurements, a monochromatic synchrotron beam illuminates the monolayer at an incident angle slightly below the critical angle of the air/water interface. The intensity of the scattered beam is collected with a position sensitive linear detector perpendicular to the monolayer surface at an azimuth angle near the incidence plane ($q_{||} \sim 0.03$ Å$^{-1}$). GIXOS signals can be collected without moving the detector in specular geometry, which offers a special advantage over XRR. This reduces the radiation time by a factor of 100 and thus minimizes the radiation damage. In case in-plane momentum transfer is very small ($q_{||} \sim 0$) and interface roughness is conformal, the measured diffuse intensity is connected to the corresponding reflectivity curve [28]. This enables one to detect conformational changes in glycans from the electron density profiles in the presence and absence of $Ca^{2+}$ [29,30]. However, the GIXOS/XRR merely yields the electron density profile but not "ion specific" density profiles.

One experimental breakthrough to get insight into the electrostatics of soft, charged interfaces is grazing-incidence X-ray fluorescence (GIXF) [31•,32]. In GIXF measurements, the monolayer is illuminated at incidence angles $\alpha_i$ below and above the critical angle of total reflection, $\alpha_c$. At $\alpha_i < \alpha_c$, the illuminated volume significantly depends on $\alpha_i$, since the penetration depth of the evanescent field is given by:

$$\Lambda(\alpha_i) = \frac{\lambda_{\text{X-ray}}}{\sqrt{8\pi}} \left[ \sqrt{\left(\alpha_i^2 - \alpha_c^2\right)^2 + 4\beta^2} - \left(\alpha_i^2 - \alpha_c^2\right) \right]^{-\frac{1}{2}}. \quad (6)$$

$\lambda_{\text{X-ray}}$ is the wavelength of the incident beam, and $\beta$ the imaginary part of the refractive index $n = 1 - \delta + i\beta$. On the other hand, the incidence beam penetrates into the bulk at $\alpha_i > \alpha_c$. The fluorescence intensity collected as a function of $\alpha_i$ yields the density profiles of target element/ions:

$$I^{flu}(\alpha_i) \sim \int_0^\infty I^{ill}(z, \alpha_i)\, c_j(z)\, \exp(-z/L_i)\, dz. \quad (7)$$

$c_j(z)$ is the concentration of element $j$ at a depth $z$ and $L_i$ is the attenuation length of water. It should be pointed out that parallel GIXOS/XRR measurements are necessary for quantitative calculations,

since the illumination profile $I^{ill}(z,\alpha_i)$ in ultrathin films significantly depends on the electron density (and thus the scattering length density $\delta$) of each layer. The combination of GIXOS/XRR and GIXF opens a new potential to determine not only ion density profiles with high accuracy [33••] but also the lateral density of recombinant proteins bound to the membrane surface (Fig. 5) [34].

### 3.2. Physical roles of glycans (2): mechanics

Glycans on membrane surfaces are specifically recognized not only by carbohydrate-binding receptors but also by complementary carbohydrates expressed in inter-cellular communication, such as the cell aggregation via homophilic interactions during embryonic development [35]. However, the influence of glycans on mechanics of interacting membranes, such as inter-membrane potentials and bending rigidity, have hardly been studied in a quantitative manner.

X-ray and neutron scattering techniques have been widely used to investigate the physical characteristics of biological membranes. Especially, specular and off-specular scattering of stacks of planar membranes offers a unique advantage over commonly used powder diffraction experiments of lipid suspensions, as the planar geometry of supported membranes enables one to identify in-plane and out-of-plane momentum transfers [36••,37•,38,39]. Experiments at controlled humidity enable one to examine the influence of the disjoining pressure on the inter-membrane interactions, while experiments in bulk buffers (i.e., in the absence of external osmotic stress) reveal the effect of solute molecules (e.g. ions, co-solvents) on membrane mechanics (Fig. 6).

In kinematic approximation, the scattering from periodical membrane stacks which possess correlated roughness can be expressed as a function of the displacement correlation function $g_k(r)$ [40••]:

$$S\left(q_z, q_{||}\right) \propto \frac{1}{q_z^2}\left[N\int_{-\infty}^{\infty} e^{-q_z^2 g_0(r)/2} e^{-iq_{||}r}dr + 2\sum_{k=1}^{N}(N-k)\cos(kq_z d)\int_{-\infty}^{\infty} e^{-q_z^2 g_k(r)/2} e^{-iq_{||}r}dr\right],$$

$$\text{where } g_k(r) = \frac{d^2}{\pi^2}\eta_C \int_{2\pi/R}^{\infty} \frac{\left[1-J_o\left(q_{||}r\right)\exp\left(-\lambda_D k q_{||}^2 d\right)\right]}{q_{||}\sqrt{1+\frac{\lambda_D^2 d^2}{4}q_{||}^4}}dq_{||}. \tag{8}$$

$g_k(r)$ can be characterized by de Gennes parameter $\lambda_D$ and Caillé parameter $\eta_C$. Here, binding/unbinding transition of interacting membranes in the perpendicular direction can generally be described as Peierls–Landau instability.

Within the framework of the discrete smectic Hamiltonian [41•], the vertical inter-membrane interaction potential is characterized by the compression modulus $B$, and the bending elasticity of the membranes by the membrane bending modulus $\kappa$:

$$H = \int_A d^2 r \sum_{n=1}^{N-1}\left(\frac{B}{2d}\left(u_{n+1}-u_n\right)^2 + \frac{\kappa}{2}\left(\nabla_{xy}^2 u_n\right)^2\right). \tag{9}$$

$N$ is the total number of membranes, $d$ the equilibrium distance, $A$ the covered area, and $u_n$ the local out-of-plane displacement of the $n^{th}$ membrane from its average vertical position. It should be noted that two key parameters in the displacement correlation function, $\lambda$ and Caillé parameter $\eta$, are directly correlated to $B$ and $\kappa$: $\eta_C \propto 1/\sqrt{\kappa B}$ and $\lambda_D = \sqrt{\kappa/B}$. Therefore, the simulation of the scattering signal enables one to determine the mechanical properties of the membranes. The specular/off-specular scattering of multilayers of glycolipids, ranging from synthetic glycolipids [42,43] to LPSs purified from bacterial mutant strains [44•], is a straightforward strategy to physically model influences of molecular chemistry, solute molecules, and genetic mutation of membrane-bound glycans on $B$ and $\kappa$.

## 4. Control of biological cells with tailor-made material interfaces

A natural extension of this field is to understand how livings cells and tissues would feel their environments via soft interfaces. In the last decades, an increasing number of studies also provided compelling evidence that biological cells have the capability of sensitively responding not only to their biochemical environment but also to their mechanical environment [45••]. These findings strongly suggest that the design of tailor-made, soft interfaces is essential for the mechanistic understanding of cellular functions as well as for the control of cells via distinct commands.

### 4.1. Dynamic cell morphology with supported membranes

Owing to the excellent capability to minimize the non-specific protein adsorption and cell adhesion, supported membrane systems have been used as the model of surrogate cell surfaces to study a variety of cellular processes, such as formation of inflammatory reactions of T-cells [5,46••]. If one utilizes recombinant proteins or ligand molecules "tagged" with biotin and histidine tags, one can easily functionalize supported membranes simply by incorporation of anchor lipids. A special interest exists in utilizing supported membranes as quantitative in vitro models to discriminate different cell phenotypes that were genetically/epigenetically modified by diseases and development.

For example, the growth and metastasis of tumors are highly dynamic processes that are regulated by the interaction of hyaluronic acid (HA) with glycoprotein CD44 [47]. In fact, enzymatic degradation

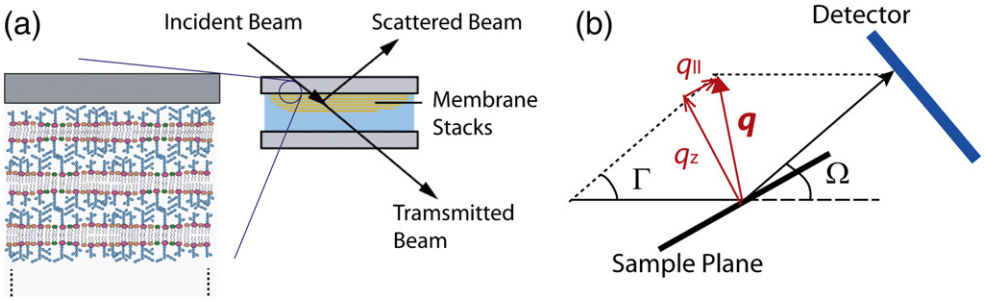


**Fig. 6.** (a) Stacks of membranes coupled to carbohydrate head groups on planar supports (supported multilayers) as the model of cell–cell contacts mediated by carbohydrates. (b) Owing to the planar geometry, the momentum transfers parallel and perpendicular to the membrane surface can easily be identified.

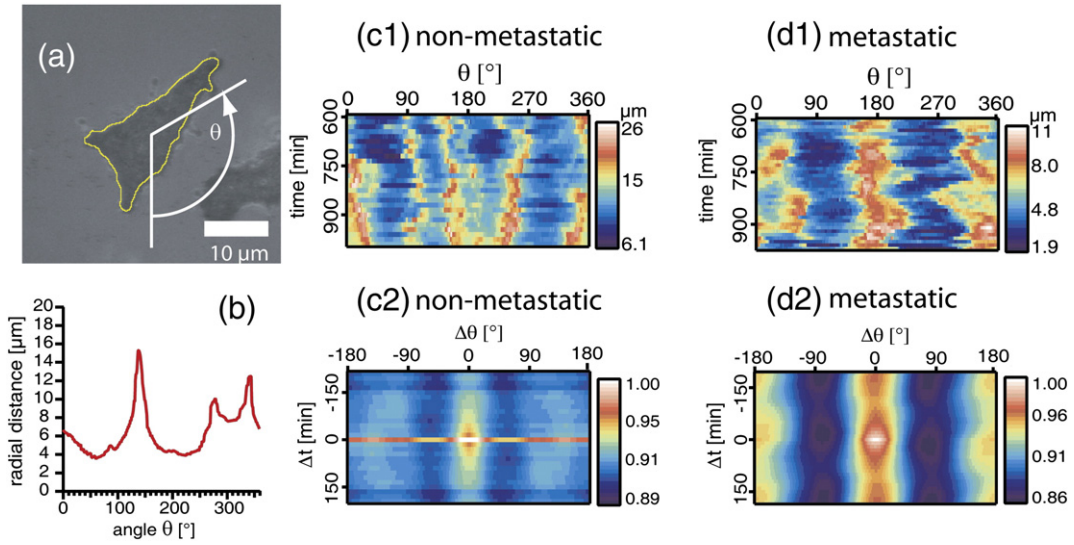


**Fig. 7.** (a) A snap shot of a pancreatic cancer cell on an oligo-HA-functionalized membrane captured by micro-interferometry. The peripheral edge of the cell was determined by the contrast in pixel intensity. (b) The amplitude of fluctuation amplitude $R(\theta,t) = r(\theta,t) - \langle r(\theta,t)\rangle_\theta$ plotted as a function of $\theta$. $\langle r(\theta,t)\rangle_\theta$ is the mean radial distance over $\theta = 0$–$360°$. Amplitude $R(\theta,t)$ map of representative (c1) non-metastatic and (d1) metastatic cancer cells plotted as function of θ recorded over time. The corresponding autocorrelations are presented in panel (c2) and (d2), respectively.

of poly-HA and accumulation of oligo-HA are associated with poor patient prognosis, which causes the increase in tumor proliferation, invasion, and angiogenesis. To mechanistically understand how CD44-HA interactions physically influence cancer metastasis, supported membranes displaying oligo-HA at defined surface densities can be used as a well defined in vitro model of surrogate cell surfaces [48•]. Such model systems allow the discrimination of phenotypes expressing different CD44 variants by measuring the area of tight adhesion zones using non-invasive reflection interference contrast microscopy [49]. Moreover, by calculating autocorrelation functions of the fluctuation amplitude of cell rims [50], it is possible to distinguish a difference in spatio-temporal patterns of metastatic and non-metastatic cancer cells hidden behind the stochastic noise of dynamic cell morphology [49]. Thus, the combination of quantitatively functionalized soft interfaces and statistical image analysis can potentially be used as a complementary tool to molecular biology readouts, which in turn will identify new routes for therapeutic intervention (Fig. 7).

### 4.2. Active control of cell fate with smart materials

Towards the "active" control of interactions at biological interfaces, one of the sophisticated approaches would be the use of polymers whose properties can be modulated by external stimuli. For example, Okano and his co-workers demonstrated non-invasive detachment of cell sheets from substrates using thermo-responsive, low critical solution temperature polymers, such as poly(N-isopropylacrylamide) [51].

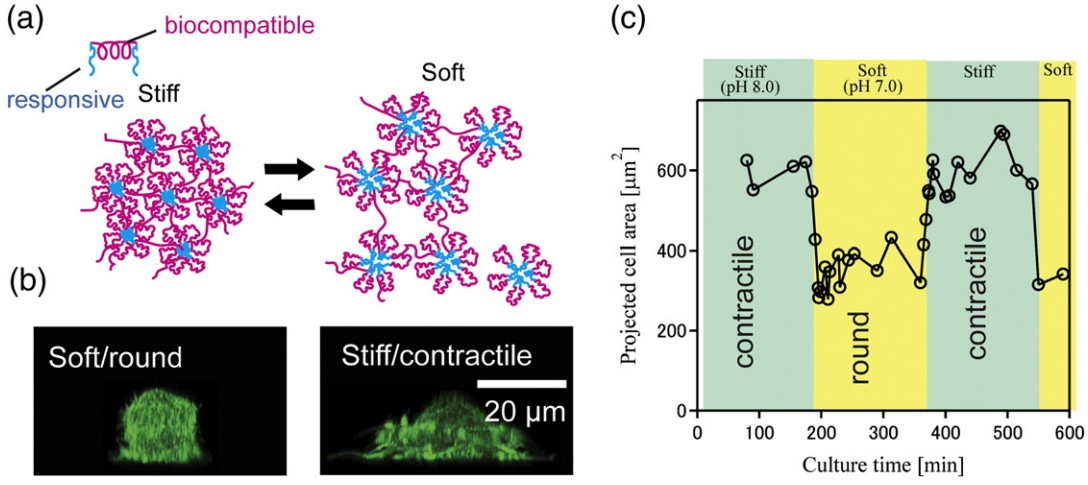


**Fig. 8.** (a) Physical gels based on triblock copolymer micelles that undergo reversible mechanical transitions. (b) Confocal fluorescence images obtained for cardiac myoblast cells on soft ($E = 1.4$ kPa, left) and stiff ($E = 40$ kPa) after 24 h, showing a clear difference in the cell morphology. (d) Dynamic switching between round and contractile morphology in response to time-dependent mechanical cues.

The cell monolayers can be harvested in a non-invasive manner and can be transplanted to the host tissue directly [52]. However, the switching via low critical salvation temperature has been limited to detach confluent cell layers from the substrate, as cell viability may significantly be interfered over time by changes in temperature. One possible solution is the use of physical gels that can reversibly change the physical properties (hydrophilicity, degree of ionization, etc.) near physiological conditions (Fig. 8). The reversible switching of polymer conformation and hence the mechanical properties can be used as time-dependent cues to influence the morphology [53••]. Changes in the cell morphology and thus remodeling of cytoskeleton induced by an abrupt change in the mechanical properties of substrates may activate cell signaling pathways, which potentially allows for the dynamic regulation of the differentiation of stem cells [54,55].

## 5. Conclusions, perspectives

The unique combination of well defined model systems and experimental techniques in real- and reciprocal space offers possibilities to investigate the physics of complex biological interfaces. Quantitative understanding of interplays of generic and specific interactions enables one to apply such systems in versatile directions, such as the regulation of the fate of cells and cell ensembles using spatio-temporal cues and design of novel sensor materials by transferring membranes and proteins onto solid-based devices.

## Acknowledgement

The author thanks all the post-doc and graduate students for their enormous contributions, especially, F. Rossetti, S. Kaufmann, R. Oliveira, E. Schneck, T. Kaindl, P. Seitz, H. Yoshikawa, W. Abuillan, A. Körner, T. Schubert, O. Purrucker, F. Rehfeldt, and M. Tutus. The author also appreciates the collaborating partners, R. Schmidt, C. Gege, R. Jordan, K. Brandenburg, D.A. Pink, J.P. Sleeman, I.M. Weiss, A.D. Ho, and S.P. Armes for their tackling of common scientific problems. The author is thankful to ESRF and ILL for the synchrotron and neutron beam times and to staff scientists, O. Konovalov and B. Demé, for the supports. The works of the author's group presented in this review were supported by the German Science Foundation (SFB 873), BMBF, JSPS, and Humboldt Foundation. The author is a member of the German Excellence Cluster “Cell Network” and Helmholtz Program “BioInterface”. The iCeMS is supported by World Premier International Research Center Initiative (WPI), MEXT, Japan.

## References and recommended reading*,**

[1] Hardt SL. Rates of diffusion controlled reactions in one, two and three dimensions. Biophys Chem 1979;10:239–43.
[2] Derjaguin BV, Churaev NV. Surface forces. New York: Consultants Bureau; 1987 .
[3] Langevin D. Dynamics of surfactant layers. Curr Opin Colloid Interface Sci 1998;3:600–7.
[4] Reiter G, Sharma A, Casoli A, David MO, Khanna R, Auroy P. Thin film instability induced by long-range forces. Langmuir 1999;15:2551–8.
[5•] Brian AA, McConnell HM. Allogeneic stimulation of cytotoxic T cells by supported planar membranes. Proc Natl Acad Sci U S A 1984;81:6159–63.First report on supported membranes, used for the stimulation of T-cells
[6•] Sackmann E. Supported membranes: scientific and practical applications. Science 1996;271:43–8.Comprehensive review on solid-supported membranes.
[7] Groves JT, Dustin ML. Supported planar bilayers in studies on immune cell adhesion and communication. J Immunol Methods 2003;278:19–32.
[8•] Tanaka M, Sackmann E. Polymer-supported membranes as models of the cell surface. Nature 2005;437:656–63.Review summarizing the progress of polymer-supported membranes.
[9] Wagner ML, Tamm LK. Tethered polymer-supported planar lipid bilayers for reconstitution of integral membrane proteins: silane-polyethylenglycol-lipid as a cushion and covalent linker. Biophys J 2000;79:1400–14.
[10] Brochard-Wyart F, de Gennes PG. Dynamics of partial wetting. Adv Colloid Interface Sci 1992;39:1–11.
[11] Tanaka M, Rehfeldt F, Schneider MF, Mathe G, Albersdörfer A, Neumaier K, et al. Wetting and dewetting of extracellular matrix and glycocalix models. J Phys Condens Matter 2005;17:S649–63.
[12•] Saffman PG, Delbrück M. Brownian motion in biological membranes. Proc Natl Acad Sci U S A 1975;72:3111–3.Theory of translational diffusion of proteins using a continuum approach.
[13] Criado M, Vaz WLC, Barrantes FJ, Jovin TM. Translational diffusion of acetylcholine receptor (monomeric and dimeric forms) of *Torpedo marmorata* reconstituted into phospholipid bilayers studied by fluorescence recovery after photobleaching. Biochemistry 1982;21:5750–5.
[14•] Evans E, Sackmann E. Translational and rotational drag coefficients for a disk moving in a liquid membrane associated with a rigid substrate. J Fluid Mech 1988;194:553–61.Modification of continuum theory taking frictional coupling into consideration.
[15•] Purrucker O, Förtig A, Jordan R, Sackmann E, Tanaka M. Control of frictional coupling of transmembrane cell receptors in model cell membranes with linear polymer spacers. Phys Rev Lett 2007;98:078102.Experimental work quantifying the frictional stress exerted to proteins.
[16] Israelachvili JN. Intermolecular and surface forces. London: Academic Press; 2007 .
[17•] Leikin S, Parsegian VA, Rau DC, Rand RP. Hydration forces. Annu Rev Phys Chem 1993;44:369–95.Comprehensive review on hydration forces.
[18•] Helfrich W. Steric interaction of fluid membranes in multilayer systems. Z Naturforsch 1978;33a:305.Theory of thermal undulation forces in multilayers.
[19] Gompper G, Kroll DM. Steric Interactions in multimembrane systems: a Monte Carlo study. Europhys Lett 1989;9:59.
[20] Seitz PC, Reif MD, Konovalov O, Jordan R, Tanaka M. Modulation of substrate–membrane interactions by linear poly(2-methyl-2-oxazoline) spacers revealed by x-ray reflectivity and ellipsometry. Chem phys chem 2009;10:2876–83.
[21•] Tanaka M, Kaufmann S, Nissen J, Hochrein M. Orientation selective immobilization of human erythrocyte membranes on ultrathin cellulose films. Phys Chem Chem Phys 2001;3:4091–5.First report on native supported membranes.
[22] Cassier T, Sinner A, Offenhäuser A, Möhwald H. Homogeneity, electrical resistivity and lateral diffusion of lipid bilayers coupled to polyelectrolyte multilayers. Colloids Surf B Biointerfaces 1999;15:215–25.
[23] Seantier B, Breffa C, Félix O, Decher G. In situ investigations of the formation of mixed supported lipid bilayers close to the phase transition temperature. Nano Lett 2003;4:5–10.
[24] Tanaka M, Wong AP, Rehfeldt F, Tutus M, Kaufmann S. Selective deposition of native cell membranes on biocompatible micro-patterns. J Am Chem Soc 2004;126:3257–60.
[25] Gabius HJ, Gabius S. Glycoscience. Chapmann & Hall: Weinheim; 1997 .
[26] Raman R, Raguram S, Venkataraman G, Paulson JC, Sasisekharan R. Glycomics: an integrated systems approach to structure–function relationships of glycans. Nat Methods 2005;2:817–24.
[27] Spitznagel JK. The effects of mammalian and other cationic polypeptides on the cytochemical character of bacterial cells. J Exp Med 1961;114:1063–78.
[28•] Mora S, Daillant J, Luzet D, Struth B. X-ray surface scattering investigation of Langmuir films: phase transitions and elastic properties. Europhys Lett 2004;66:694–700.Paper describing the principle of GIXOS measurements.
[29] Oliveira RG, Schneck E, Quinn B, Konovalov O, Brandenburg K, Gutsmann T, et al. Crucial roles of charged saccharide moieties in survival of Gram negative bacteria against protamine revealed by combination of grazing incidence X-ray structural characterizations and Monte Carlo simulations. Phys Rev E 2009;81:041901.
[30] Oliveira RG, Schneck E, Quinn B, Konovalov O, Gill T, Hanna CB, et al. Physical mechanism of bacterial survival revealed by combined grazing-incidence x-ray scattering and Monte Carlo simulation. C R Chimie 2009;12:209–17.
[31•] Yun WB, Bloch JM. X-ray near total external fluorescence method: experiment and analysis. J Appl Phys 1990;68:1421–8.Pioneering work on GIXF at soft interfaces.
[32] Novikova NN, Yurieva EA, Zheludeva SI, Kovalchuk M, Stepina N, Tolstikhina A, et al. X-ray fluorescence methods for investigations of lipid/protein membrane models. J Synchrotron Radiat 2005;12:511–6.
[33•] Schneck E, Schubert T, Konovalov OV, Quinn BE, Gutsmann T, Brandenburg K, et al. Quantitative determination of ion distributions in bacterial lipopolysaccharide membranes by grazing-incidence X-ray fluorescence. Proc Natl Acad Sci U S A 2010;107:9147–51.Precise localization of mono- and divalent cations near biological interfaces.
[34] Abuillan W, Vorobiev A, Hartel A, Jones NG, Engstler M, Tanaka M. Quantitative determination of the lateral density and intermolecular correlation between proteins anchored on the membrane surfaces using grazing incidence small-angle X-ray scattering and grazing incidence X-ray fluorescence. J Chem Phys 2012;137:204907–8.
[35] Eggens I, Fenderson B, Toyokuni T, Dean B, Stroud M, Hakomori S. Specific interaction between Lex and Lex determinants. A possible basis for cell recognition in preimplantation embryos and in embryonal carcinoma cells. J Biol Chem 1989;264:9476–84.
[36•] Safinya CR, Roux D, Smith GS, Sinha SK, Dimon p, Clark NA, et al. Steric interactions in a model multimembrane system: a synchrotron X-ray study. Phys Rev Lett 1986;57:2718–21.Pioneering works on off-specular scattering of lipid membrane stacks.
[37•] Salditt T. Structure and fluctuations of highly oriented phospholipid membranes. Curr Opin Colloid Interface Sci 2000;5:19–26.Comprehensive review on the modern scattering techniques for lipid membranes.
[38] Katsaras J. Highly aligned lipid membrane systems in the physiologically relevant “excess water” condition. Biophys J 1997;73:2924–9.
[39] Liu Y, Nagle JF. Diffuse scattering provides material parameters and electron density profiles of biomembranes. Phys Rev E 2004;69:040901.

* of special interest.
** of outstanding interest.

[40••] Sinha SK. X-Ray Diffuse-Scattering as a probe for thin-film and interface structure. J Phys III 1994;4:1543–57.Theoretical framework to describe scattering functions from rough surfaces.
[41•] Lipowsky R, Leibler S. Unbinding transitions of interacting membranes. Phys Rev Lett 1986;56:2541–4.Important paper describing binding/unbinding transition of membranes. Note that the bending rigidity values in this paper was corrected by a factor of 10 in an erratum.
[42] Schneck E, Rehfeldt F, Oliveira RG, Gege C, Demé B, Tanaka M. Modulation of intermembrane interaction and bending rigidity of biomembrane models via carbohydrates investigated by specular and off-specular neutron scattering. Phys Rev E 2008;78:061924.
[43] Schneck E, Deme B, Gege C, Tanaka M. Membrane adhesion via homophilic saccharide–saccharide interactions investigated by neutron scattering. Biophys J 2011;100:2151–9.
[44•] Schneck E, Oliveira RG, Rehfeldt F, Demé B, Brandenburg K, Seydel U, et al. Mechanical properties of interacting lipopolysaccharide membranes from bacteria mutants studied by specular and off-specular neutron scattering. Phys Rev E 2009;80:041929.Paper demonstrating the application of off-specular scattering to membranes of complex lipopolysaccharides.
[45••] Discher DE, Janmey P, Wang Y-L. Tissue cells feel and respond to the stiffness of their substrate. Science 2005;310:1139–43.Comprehensive review on mechano-sensing of cells.
[46••] Grakoui A, Bromley SK, Sumen C, Davis MM, Shaw AS, Allen PM, et al. The immunological synapse: a molecular machine controlling T cell activation. Science 1999;285:221–7.Ground-breaking paper describing the immunological synapse pattern formation.
[47] Ponta H, Sherman L, Herrlich PA. CD44: from adhesion molecules to signalling regulators. Nat Rev Mol Cell Biol 2003;4:33–45.
[48•] Kaindl T, Rieger H, Kaschel L-M, Engel U, Schmaus A, Sleeman J, et al. Spatio-temporal patterns of pancreatic cancer cells expressing CD44 isoforms on supported membranes displaying hyaluronic acid oligomers arrays. PLoS One 2012;7:e42991.Combination of supported membranes, micro-interferometry, and statistical physics tool.
[49] Zilker A, Engelhardt H, Sackmann E. Dynamic reflection interference contrast (RIC-) microscopy: a new method to study surface excitations of cells and to measure membrane bending elastic moduli. J Phys 1987;48:2139–51 [France].
[50] Maeda YT, Inose J, Matsuo MY, Iwaya S, Sano M. Ordered patterns of cell shape and orientational correlation during spontaneous cell migration. PLoS One 2008;3:e3734.
[51] Hirose M, Kwon OH, Yamato M, Kikuchi A, Okano T. Creation of designed shape cell sheets that are noninvasively harvested and moved onto another surface. Biomacromolecules 2000;1:377–81.
[52] Matsuda N, Shimizu T, Yamato M, Okano T. Tissue engineering based on cell sheet technology. Adv Mater 2007;19:3089–99.
[53••] Yoshikawa HY, Rossetti FF, Kaufmann S, Kaindl T, Madsen J, Engel U, et al. Quantitative evaluation of mechanosensing of cells on dynamically tunable hydrogels. J Am Chem Soc 2011;133:1367–74.Paper demonstrating the dynamic mechanosensing upon abrupt changes in the substrate elasticity.
[54] Guvendiren M, Burdick JA. Stiffening hydrogels to probe short- and long-term cellular responses to dynamic mechanics. Nat Commun 2012;3:792.
[55] Higuchi A, Ling Q-D, Chang Y, Hsu S-T, Umezawa A. Physical cues of biomaterials guide stem cell differentiation fate. Chem Rev 2013;113:3297–328.